# Formation of Porphyrin $\pi$ Cation Radical in Zinc-Substituted Horseradish Peroxidase†

Yoshiaki Kaneko,‡ Mamoru Tamura,* and Isao Yamazaki

ABSTRACT: Zinc-substituted horseradish peroxidase is oxidized by $K_2IrCl_6$ to a characteristic state which retains one oxidizing equivalent more than the zinc peroxidase. The oxidized enzyme gives an optical absorption spectrum similar to that of compound I of peroxidase and catalase, and a $g = 2$ electron paramagnetic resonance signal which has an intensity corresponding to the porphyrin content. It is reduced back to the zinc peroxidase by a stoichiometric amount of ferrocyanide or by a large excess of $K_3IrCl_6$. From the equilibrium data, the value of $E_0'$ for the zinc peroxidase couple is estimated to be 0.74 V at pH 6. The oxidized zinc peroxidase is also formed by the addition of $H_2O_2$ or upon illumination with white light. The rate constants for the oxidation by $K_2IrCl_6$ and $H_2O_2$ at pH 8.0 are $8 \times 10^5$ and $8 \times 10^2$ $M^{-1}$ $s^{-1}$, respectively. No essential spectral change can be observed when $K_2IrCl_6$ is added to the metal-free peroxidase (protoporphyrin–apoperoxidase complex) or to zinc-substituted sperm whale myoglobin.

Compound I is the primary intermediate compound formed in the reactions of peroxidase and catalase with $H_2O_2$. The chemical as well as electronic properties of compound I have drawn much interest and have been subjected to various physicochemical studies. This compound has a characteristic optical absorption spectrum of green color and retains two oxidizing equivalents above the ferric enzyme (Chance, 1952; George, 1953; Schonbaum & Lo, 1972; Yamada & Yamazaki, 1974). The Mössbauer spectroscopy (Maeda & Morita, 1967; Moss et al., 1969) showed that the iron atom of compound I is present as the ferryl state ($FeO^{2+}$), which is known to be the electronic state of iron in compound II, the secondary intermediate compound in peroxidase catalysis. Dolphin et al. (1971) showed that the optical absorption spectrum of compound I resembles the spectra of chemically synthesized porphyrin $\pi$ cation radicals. Since then, it has been accepted that the two oxidizing equivalents of compound I are shared between the iron atom as the ferryl state and the porphyrin as a $\pi$ cation radical. This view is not necessarily in conflict with EPR[1] data (Morita & Mason, 1965; Aasa et al., 1975; Schulz et al., 1979) but has been disputed on the basis of NMR data (Morishima & Ogawa, 1978). In this paper, we will report the formation of a stable free radical of porphyrin in zinc-substituted horseradish peroxidase.

## Experimental Procedures

Zinc protoporphyrin IX was synthesized by the method of Fisher & Pützer (1926) from zinc acetate and protoporphyrin IX. The crude product was subjected to silica gel column chromatography and developed with a mixed solvent of chloroform, *n*-hexane, and methanol at a volume ratio of 10:10:1. Sperm whale oxymyoglobin was prepared from the meat as previously reported (Yamazaki et al., 1964). Horseradish peroxidase was purified by DEAE- and CM-cellulose column chromatography according to Shannon et al. (1966) from a crude preparation purchased from Toyobo Co. (Osaka). The enzyme used ($A_{403nm}/A_{280nm} = 3.0$) was a main fraction (peroxidases B and C) adsorbed on a CM-cellulose column. All other reagents were analytical grade.

Zinc protoporphyrin IX was incorporated into apomyoglobin and apoperoxidase as reported previously (Tamura et al., 1972), where the zinc porphyrin was dissolved in alkaline water. After dialysis against distilled water, the zinc proteins were purified by DEAE-cellulose column chromatography in a manner similar to the purification of vanadyl myoglobin and peroxidase (Tamura et al., 1977). The concentrations of apoproteins and the zinc porphyrin were determined spectrophotometrically on the basis of the absorbance at 280 nm and the Soret peak, respectively (Leonard et al., 1974).

Optical absorption spectra were measured with Shimazu MPS-5000 and Hitachi-124 spectrophotometers. For the optical measurement, 3 mL of sample solution was used. The rate of oxidation of zinc peroxidase by $K_2IrCl_6$ was measured with a Union Giken rapid-reaction analyzer, Model RA-1300. This instrument is equipped with a flow apparatus and can be used as a sensitive photometer at a fixed wavelength. The buffer systems (80 mM) used in this experiment were sodium acetate for pH 4–5.5, Bis-Tris-HCl for pH 6–7, Tris-HCl for pH 7.5–9, and glycine–NaOH for pH 9.5–10.5. Since $K_2IrCl_6$ is known to be unstable above neutral pH, its stock solution was weakly acidified with HCl. The reactions were carried out at 20 °C.

The photooxidation was performed by illuminating the sample solution in the cell compartment of the spectrophotometer with a 30-W white lamp. The spectra of photooxidized products were measured after cessation of the illumination.

A Varian E-9 spectrometer operated with 100-kHz field modulation was used for EPR measurements. The microwave frequency and power were 9.538 GHz and 5 mW, respectively. The modulation amplitude was 10 G.

## Results

Figure 1A shows absorption spectra of zinc protoporphyrin in aqueous solutions with and without imidazole. The absorbance peaks of zinc protoporphyrin were shifted from 412, 544, and 582 nm to 425, 554, and 590 nm, respectively, upon coordination with imidazole. The spectrophotometric titration of zinc porphyrin with imidazole showed that the spectral shift might represent the formation of a 5-coordinated complex. Figure 1B shows absorption spectra of zinc myoglobin and zinc

† From the Biophysics Division, Research Institute of Applied Electricity, Hokkaido University, Sapporo 060, Japan. *Received May 6, 1980.*

‡ Present address: Nippon Kayaku Co. Ltd. Asa Laboratory, Sanyo-cho, Asa, Yamaguchi 757, Japan.

[1] Abbreviations used: EPR, electron paramagnetic resonance; NMR, nuclear magnetic resonance; CM, carboxymethyl.

0006-2960/80/0419-5795$01.00/0 

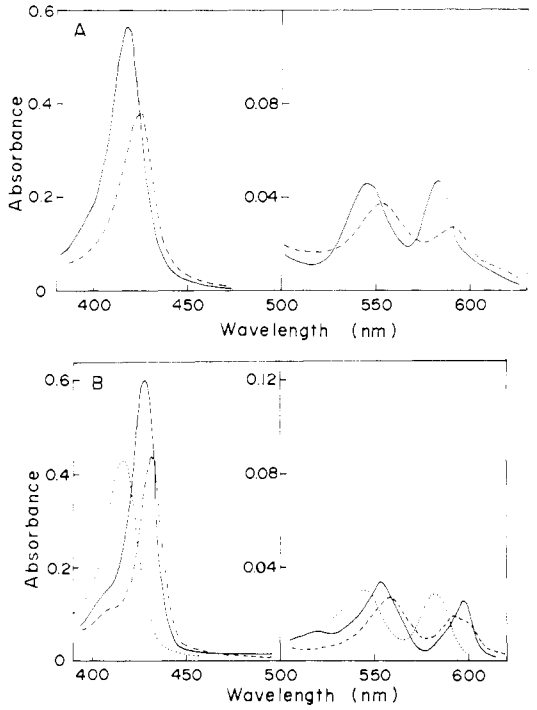


FIGURE 1: Absorption spectra of zinc protoporphyrin, zinc peroxidase, and zinc myoglobin. (A) Zinc protoporphyrin in weak alkaline water (pH 10–11, —). Imidazole (final concentration 0.1 M) was added to it, and then the pH became about 7 (---). (B) Zinc myoglobin (—) and zinc peroxidase (---) at pH 8.0. Sodium dodecyl sulfate was added to zinc myoglobin (···).

Table I: Optical Absorption Maxima[a]

| | |
|---|---|
| zinc protoporphyrin in alkaline water | 412 (87.4)[b] |
| | 544 (6.17)[b] |
| | 582 (6.01)[b] |
| zinc protoporphyrin in alkaline water with imidazole | 425 |
| | 554 |
| | 590 |
| zinc protoporphyrin in pyridine | 426 |
| | 551 |
| | 588 |
| zinc myoglobin | 429[c] |
| | 552 |
| | 596 |
| zinc peroxidase | 432 (117) |
| | 558 |
| | 592 |
| zinc peroxidase (oxidized) | 412 (38) |
| | 617 |
| | 686 (8.0) |

[a] λ, nm ($\epsilon_{mM}$). [b] Cited from Leonard et al. (1974). [c] Atassi (1967) reported values of 423 and 544 nm.

peroxidase. The spectra were somewhat similar to that of (imidazole)zinc porphyrin. Upon addition of sodium dodecyl sulfate to zinc myoglobin, the spectrum turned into the base-free zinc porphyrin. Between pH 5 and 10, the optical spectrum of zinc myoglobin did not change while small but distinct spectral changes were seen in the Soret and 600-nm bands for zinc peroxidase. Absorption maxima of zinc protoporphyrin and its derivatives are listed in Table I.

Upon addition of $K_2IrCl_6$, the spectrum of zinc peroxidase turned into a characteristic one having new bands at 410 and 686 nm. The spectrum resembled that of peroxidase compound I. No essential spectral change was seen when $K_2IrCl_6$ was added to metal-free peroxidase (protoporphyrin–apoperoxidase complex) and to zinc myoglobin. Figure 2 shows changes in the optical spectrum of zinc peroxidase upon successive additions of $K_2IrCl_6$. The isosbestic points were

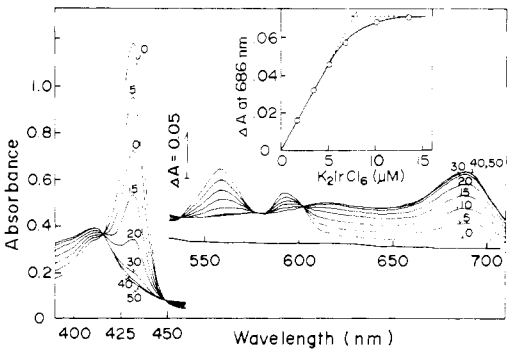


FIGURE 2: Changes in the spectrum of zinc peroxidase upon additions of $K_2IrCl_6$. An aliquot of 1 mM $K_2IrCl_6$ solution was added to 10 μM zinc peroxidase (20 mM Tris–HCl, pH 8.0), and the spectrum was measured soon after the addition. The total amount (μL) of the $K_2IrCl_6$ solution added is indicated in the figure. In the inset, the absorbance change is plotted against the concentration of $K_2IrCl_6$.

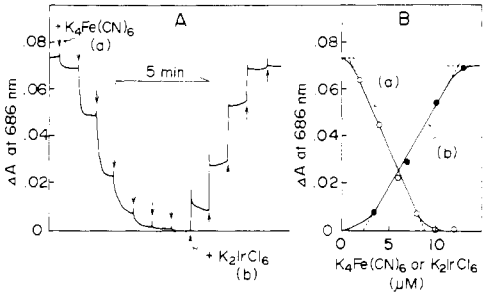


FIGURE 3: Oxidative and reductive titrations of zinc peroxidase with $K_2IrCl_2$ and $K_4Fe(CN)_6$. (A) To the oxidized zinc peroxidase (10 μM) formed by the addition of $K_2IrCl_6$ in 80 mM Tris-HCl (pH 8.0) was added 5 μL of 1.2 mM $K_4Fe(CN)_6$ solution at each arrow (a). After the 7th addition in a, 10 μL of 1.0 mM $K_2IrCl_6$ solution was added at each arrow (b). (B) The changes in absorbance at 686 nm in experiments a and b are plotted against the concentrations of $K_4Fe(CN)_6$ and $K_2IrCl_6$, respectively.

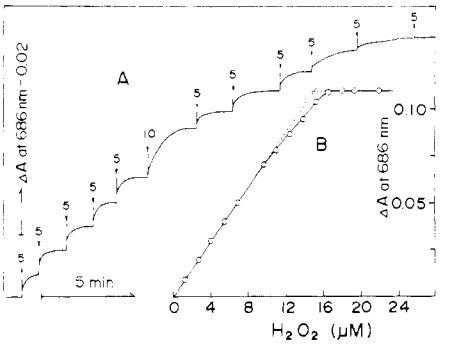


FIGURE 4: Titration of zinc peroxidase with $H_2O_2$. (A) An aliquot of 0.83 mM $H_2O_2$ solution was added to 15 μM zinc peroxidase (80 mM Tris-HCl, pH 8.0) at each arrow. The amount (μL) of the $H_2O_2$ solution added is indicated in the figure. (B) The change in absorbance at 686 nm is plotted against the concentration of $H_2O_2$.

clearly seen at 415, 448, 532, and 600 nm during the spectral transition. The spectral change could be reversed by the addition of ferrocyanide. The reversibility and stoichiometry in the oxidation and reduction of zinc peroxidase are shown in Figure 3. These results indicated that the oxidized zinc peroxidase retained about one oxidizing equivalent.

$H_2O_2$ could convert zinc peroxidase into the oxidized form, the optical spectrum of which was indistinguishable from that formed by the addition of $K_2IrCl_6$. The spectrophotometric titration showed that the oxidation occurred at a molar ratio of 1:1 (Figure 4). For the back-titration of the oxidized zinc peroxidase, only 1 mol of ferrocyanide was consumed per mol of enzyme reduced. The reaction of zinc peroxidase with $H_2O_2$

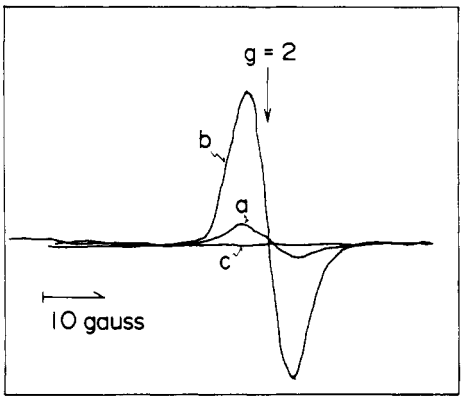


FIGURE 5: EPR spectra of zinc peroxidase: (a) 60 $\mu$M zinc peroxidase in 80 mM Tris-HCl, pH 8.0; (b) a slight excess of $K_2IrCl_6$ was added to (a); (c) an excess of $K_4Fe(CN)_6$ was added to (b).

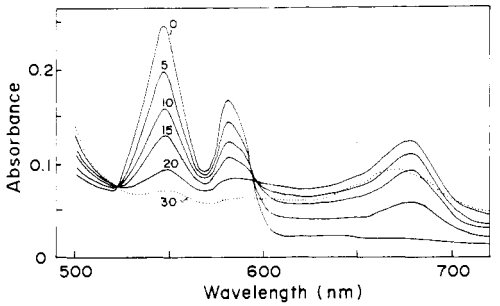


FIGURE 6: Photooxidation of zinc peroxidase. The conditions were 30 $\mu$M zinc peroxidase and 80 mM Tris-HCl, pH 8.0. The zinc peroxidase solution was illuminated with white light, and the spectrum was measured at indicated times (min). The light was off during the measurement (about 30 s).

was slow, and the second-order rate constant was measured to be $8 \times 10^2$ $M^{-1}$ $s^{-1}$ at pH 8.0.

Figure 5 shows EPR absorption spectra of zinc peroxidase and its oxidized form. The measurements were carried out at room temperature to avoid the overlap of the absorption of the metal ions. Our preparation of zinc peroxidase gave a small EPR absorption at $g = 2$. The absorption with a half-width of 10 G markedly increased upon addition of $K_2IrCl_6$. The strong signal completely disappeared upon addition of excess ferrocyanide. The weak EPR signal of our zinc peroxidase preparation also disappeared by the ferrocyanide addition. It seemed that our preparation contained a small amount of oxidized form, which was also responsible for a weak 686-nm band of the original sample in the experiment of Figure 2. The spin concentration of fully oxidized zinc peroxidase (Figure 5b) was estimated to be more than 90% of the enzyme concentration. The contamination of our zinc peroxidase preparation with its oxidized form might be explained by the following experiment.

Figure 6 shows a spectral change of zinc peroxidase when its solution was illuminated with white light at room temperature. The isosbestic points were observed during 20 min of illumination, indicating the formation of oxidized zinc peroxidase. Further illumination, however, caused a nonspecific decrease in absorbance. It was concluded from the increase in absorbance at 686 nm that approximately 60% of zinc peroxidase could be converted into the oxidized form by this method. This oxidized species was also reduced to zinc peroxidase by ferrocyanide.

The rate of oxidation of zinc peroxidase by $K_2IrCl_6$ could be measured by the stopped-flow method. Figure 7A shows such a kinetic trace measured at 430 nm. The reaction obeyed the first-order kinetics under the experimental conditions, and

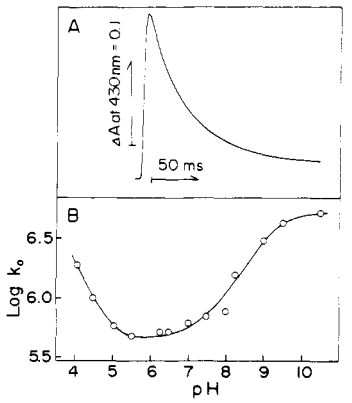


FIGURE 7: Rate constant for the oxidation of zinc peroxidase by $K_2IrCl_6$. (A) A stopped-flow trace of the absorbance at 430 nm. Two solutions of 3.0 $\mu$M zinc peroxidase with 80 mM Tris-HCl (pH 8.0) and 31 $\mu$M $K_2IrCl_6$ were mixed. (B) The logarithmic values of the second-order rate constant ($M^{-1}$ $s^{-1}$) are plotted against pH.

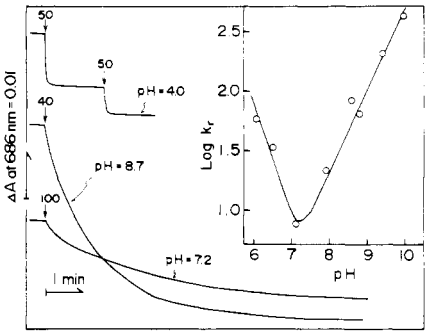


FIGURE 8: Reduction of oxidized zinc peroxidase by $K_3IrCl_6$. Aliquots of 25.2 mM $K_3IrCl_6$ solution were added to 7 $\mu$M oxidized zinc peroxidase at the arrows. The amount ($\mu$L) of the $K_3IrCl_6$ solution is indicated in the figure. In the inset, the logarithmic values of the second-order rate constant ($M^{-1}$ $s^{-1}$) are plotted against pH.

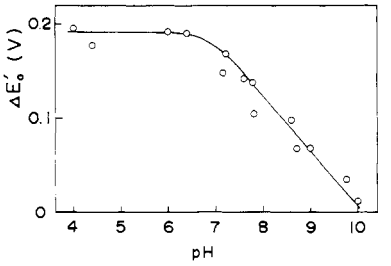


FIGURE 9: The difference $E_0'(K_2IrCl_6/K_3IrCl_6) - E_0'$(the zinc peroxidase couple) is plotted against pH. The values were calculated from the equilibrium data (see Figure 8).

the rate constant was measured to be 24.8 $s^{-1}$ at pH 8.0. The same value was obtained when the absorbance change was measured at 686 nm. Since the pseudo-first-order rate constant was proportional to the concentration of $K_2IrCl_6$, the second-order rate constant could be calculated. The rate constant was measured at various pH values, and its logarithmic value was plotted against pH in Figure 7B.

Oxidized zinc peroxidase was reduced by the addition of a large excess of $K_3IrCl_6$. The reaction was relatively slow and reached an equilibrium at times of a few seconds to 10 min, the time greatly depending on pH (Figure 8). The second-order rate constant for the reaction of oxidized zinc peroxidase with $K_3IrCl_6$ exhibited sharp pH dependence (inset of Figure 8). As the pH increased above 9, the reduction by $K_3IrCl_6$ began to be followed by the slower one. The rate constant plotted in the inset of Figure 8 was calculated from the fast phase. From equilibrium data shown in Figure 8, it was possible to calculate the difference in the oxidation–re-

duction potential between the zinc peroxidase couple and the $K_2IrCl_6$–$K_3IrCl_6$ couple. Figure 9 shows the pH dependence of $\Delta E_0'$. With $E_0'(K_2IrCl_6/K_3IrCl_6)$ = 0.93 V (Fergusson, 1956), $E_0'$ for the zinc peroxidase couple was calculated to be 0.74 V at pH 6.0. The equilibrium constant roughly equaled the ratio of rate constants for oxidation and reduction at pH 6, but the discrepancy between the two values became distinct as the pH increased.

## Discussion

The oxidative and reductive titration data in Figures 2 and 3 demonstrate that a species having an optical spectrum like that of compound I retains one oxidizing equivalent above zinc peroxidase. This is identified as a free radical by the EPR measurement. From a comparison of the optical spectrum of oxidized zinc peroxidase with that of chemically synthetic compounds (Dolphin et al., 1971), we conclude that the EPR signal we observed is consistent with a $\pi$ cation radical of porphyrin. It is of interest to note that the 600–700-nm spectrum of oxidized zinc peroxidase resembles that of catalase compound I rather than peroxidase compound I.

Lack of the paramagnetic center in zinc peroxidase makes it possible to show a sharp EPR signal with about one spin/enzyme. The presence of iron may obscure quantitation of the EPR signal of peroxidase compound I as can be seen in the results reported by Aasa et al. (1975) and Schulz et al. (1979). Morishima & Ogawa (1978) have reported NMR data which provide evidence against a porphyrin cation radical and a low-spin iron(IV) in peroxidase compound I. However, La Mar & De Ropp (1980) have concluded that the NMR spectrum of deutero-horseradish peroxidase compound I is inconsistent with the formulation of Morishima & Ogawa which involves a high-spin iron(IV) and an amino acid radical and also that a porphyrin cation radical cannot be excluded. La Mar & De Ropp (1980) have also stated that the dramatically different hyperfine shift patterns in compounds I and II of peroxidase can be taken as evidence for an additional source of unpaired spin density at the heme periphery, namely, the cation radical. It is therefore important to confirm if similar hyperfine shifts appear upon the oxidation of zinc peroxidase.

Zinc peroxidase still possesses reactivity toward $H_2O_2$ and is oxidized by $H_2O_2$ to the radical form. The stoichiometry in the reaction between $H_2O_2$ and ZnHRP is 1:1, and the fate of one of the two oxidizing equivalents of $H_2O_2$ is not characterized yet. In this sense, the reaction appears to resemble the oxidation of metmyoglobin by $H_2O_2$ (George & Irvine, 1952) in which one oxidizing equivalent of $H_2O_2$ is used to oxidize the ferric iron to the ferryl form and the fate of one more equivalent is not known. It should be noted here that the rate constant for the reaction of zinc peroxidase with $H_2O_2$ is about $^1/_{10\,000}$ of that for the reaction of the native enzyme with $H_2O_2$. It is of primary importance that the protoporphyrin–apoperoxidase complex is not oxidized by $H_2O_2$ and $K_2IrCl_6$. It may be concluded that the metal ion in the porphyrin ring plays a role in the formation and stabilization of the porphyrin $\pi$ cation radical and particularly that the ferric ion participates in the catalytic cleavage of the O–O bond in addition to the role of retaining one oxidizing equivalent.

The two-step oxidation of horseradish peroxidase to compound I via compound II was first suggested by George (1953). This was recently confirmed by three laboratories (Hayashi & Yamazaki, 1979; Hewson & Hager, 1979a,b; Nadezhdin & Dunford, 1979). The rate constant for the reaction between zinc peroxidase and $K_2IrCl_6$ is $8 \times 10^5$ $M^{-1}$ $s^{-1}$ at pH 8. This value is about 10 and 1000 times higher than the respective values for the oxidations of compound II and the ferric form of horseradish peroxidase by $K_2IrCl_6$ (Hayashi & Yamazaki, 1979). The results indicate that the iron atom of heme does not directly participate in the electron-transfer reaction from the enzyme to $K_2IrCl_6$. It seems that the intermolecular electron transfer occurs at the periphery of the porphyrin ring. From these kinetic data and also from the fact that the oxidation potential of compound II is higher by 230 mV than that of zinc peroxidase (Hayashi & Yamazaki, 1979), it can be said that the electron removal from the porphyrin ring of compound II is retarded by the presence of the ferryl ion.

Molecular oxygen may be a candidate for the oxidant in the formation of $\pi$ cation radical in zinc peroxidase by illumination. This fact explains the appearance of a weak EPR signal and a weak absorbance at 686 nm in our preparation of zinc peroxidase. In spite of its high oxidation–reduction potential, the porphyrin $\pi$ cation radical is fairly stable in the heme pocket of horseradish peroxidase. Although metmyoglobin is oxidized by $K_2IrCl_6$ to the ferryl form (George & Irvine, 1954), the cation radical cannot be formed in zinc myoglobin. This must be a characteristic difference reflecting the structure of the heme pocket between peroxidase and myoglobin.

## Acknowledgments

We thank Professor Hiroshi Yoshida and Dr. Masaki Ogasawara, Faculty of Engineering, Hokkaido University, for the use of a Varian E-9 EPR spectrometer.

## References

Aasa, R., Vanngård, T., & Dunford, H. B. (1975) *Biochim. Biophys. Acta 391*, 259.
Atassi, M. Z. (1967) *Biochem. J. 103*, 29.
Chance, B. (1952) *Arch. Biochem. Biophys. 41*, 416.
Dolphin, D., Forman, A., Borg, D. C., Fajer, K., & Felton, R. H. (1971) *Proc. Natl. Acad. Sci. U.S.A. 68*, 614.
Fergusson, R. R. (1956) *J. Am. Chem. Soc. 78*, 741.
Fisher, H., & Pützer, B. (1926) *Hoppe-Seyler's Z. Physiol. Chem. 154*, 39.
George, P. (1953a) *Biochem. J. 54*, 267.
George, P. (1953b) *Science (Washington, D.C.) 117*, 220.
George, P., & Irvine, D. H. (1952) *Biochem. J. 52*, 511.
George, P., & Irvine, D. H. (1954) *Biochem. J. 58*, 188.
Hayashi, Y., & Yamazaki, I. (1979) *J. Biol. Chem. 254*, 9101.
Hewson, W. D., & Hager, L. P. (1979a) *J. Biol. Chem. 254*, 3175.
Hewson, W. D., & Hager, L. P. (1979b) *J. Biol. Chem. 254*, 3182.
La Mar, G. N., & De Ropp, J. S. (1980) *J. Am. Chem. Soc. 102*, 395.
Leonard, J. J., Yonetani, T., & Gallis, J. B. (1974) *Biochemistry 13*, 1460.
Maeda, S., & Morita, Y. (1967) *Biochem. Biophys. Res. Commun. 29*, 689.
Morishima, I., & Ogawa, S. (1978) *Biochemistry 17*, 4384.
Morita, Y., & Mason, H. S. (1965) *J. Biol. Chem. 240*, 2654.
Moss, T. H., Ehrenberg, A., & Bearden, A. J. (1969) *Biochemistry 8*, 4159.
Nadezhdin, A., & Dunford, H. B. (1979) *Can. J. Biochem. 57*, 1080.
Schonbaum, G. R., & Lo, S. (1972) *J. Biol. Chem. 247*, 3353.
Schulz, C. E., Devaney, P. W., Winkler, H., Debrunner, P. G., Doan, N., Chiang, R., Rutter, R., & Hager, L. P. (1979) *FEBS Lett. 103*, 102.
Shannon, L. M., Kay, E., & Lew, J. Y. (1966) *J. Biol. Chem. 241*, 2166.

Tamura, M., Asakura, T., & Yonetani, T. (1972) *Biochim. Biophys. Acta 268*, 292.
Tamura, M., Shimizu, N., & Hayashi, K. (1977) *Biochem. Biophys. Res. Commun. 75*, 1029.
Yamada, H., & Yamazaki, I. (1974) *Arch. Biochem. Biophys. 165*, 728.
Yamazaki, I., Yokota, K., & Shikama, K. (1964) *J. Biol. Chem. 239*, 4151.

# Substrate Specificity of Two Chymotrypsin-like Proteases from Rat Mast Cells. Studies with Peptide 4-Nitroanilides and Comparison with Cathepsin G†

Norio Yoshida, Michael T. Everitt, Hans Neurath, Richard G. Woodbury, and James C. Powers*

ABSTRACT: The substrate specificity of chymotrypsin-like enzymes from typical mast cells, rat mast cell protease I (RMCP I), and from atypical mast cells, rat mast cell protease II (RMCP II), has been investigated with peptide 4-nitroanilide (NA) substrates and peptide chloromethyl ketone inhibitors. Suc-Phe-Pro-Phe-NA and Suc-Phe-Leu-Phe-NA are the best substrates for both RMCP I and RMCP II. In the case of RMCP II, both the $P_3$ (Phe) and the $P_4$ [succinyl (Suc)] groups are important. Succinyl tetrapeptides with nearly the same sequence were not as sensitive to either rat protease. The pH optimum of the hydrolysis of Suc-Phe-Leu-Phe-NA by RMCP II was pH 6.6 and by RMCP I was ca. pH 8.5. The $S_2$ subsite of RMCP II prefers Thr over either Leu or Pro. The subsite specificity of RMCP II may be explained on the basis of interaction with Asn-86 in $S_2$, a hydrophobic $S_3$ subsite due to the presence of Phe-178, and at pH 6.6, an interaction with a cationic His-200 in the $S_4$ subsite. Suc-Phe-Pro-Phe-NA is the best 4-nitroanilide substrate yet found for cathepsin G. The observed subsite preferences indicate that the $S_3$ and $S_4$ subsites of RMCP I, RMCP II, and cathepsin may be very similar. The $k_{cat}/K_M$ values of RMCP II and cathepsin G are significantly lower than those observed with bovine chymotrypsin, RMCP I, and other serine proteases. It is not clear whether this difference is related to their physiological function or is due to a non-optimum substrate structure. Prolyl residues at the $P_2$ position enhance the effectiveness of substrates and inhibitors for RMCP I, RMCP II, and cathepsin G. Unlike other serine proteases, both rat enzymes can also accept Pro residues in position $P_3$ of substrates. A peptide chloromethyl ketone, Suc-Pro-Leu-Phe$CH_2$Cl, was synthesized in order to take advantage of this phenomenon. This compound is an effective inhibitor of RMCP I. RMCP I is inhibited 10–93 times faster than RMCP II, cathepsin G, or bovine chymotrypsin. This inhibitor may be useful in elucidating the physiological function of RMCP I and RMCP II.

A number of intracellular chymotrypsin-like serine proteases have recently been isolated and characterized. These include a protease from rat small intestine (Katunuma et al., 1975), from rat skeletal muscle (Katunuma et al., 1975; Everitt & Neurath, 1979), and from human leukocyte cathepsin G. The protease from rat small intestine has been shown by immunofluorescent studies to be localized in atypical mast cells of the mucosa (Woodbury et al., 1978c) whereas the rat skeletal muscle enzyme is derived from typical mast cells (Woodbury et al., 1978b). The protease from typical mast cells is the same as the peritoneal mast cell protease, chymase, described by Benditt & Arase (1959). To distinguish the enzymes, the protease from typical mast cells is referred to as rat mast cell protease I (RMCP I),[1] and that from atypical cell is designated rat mast cell protease II (RMCP II). Cathepsin G is located in leukocyte granules.

The complete amino acid sequence of RMCP II has been determined and shows 33% identity with bovine chymotrypsin (Woodbury et al., 1978a). The catalytic triad of chymotrypsin is maintained in RMCP II, but there are a number of amino acid changes in the region of the primary and extended substrate binding sites. Although the primary structure of RMCP I is not complete, the two rat enzymes show 75% homology in the first 51 amino acid residues (Woodbury et al., 1978b). Comparison of the N-terminal 21 amino acid residues of cathepsin G with RMCP I and RMCP II reveals 4 and 6 changes, respectively.

The substrate specificity of both rat proteases has been studied by using natural peptide substrates such as glucagon and the oxidized insulin B chain (Kobayashi et al., 1978; Kobayashi & Katunuma, 1978). Both enzymes cleaved peptide bonds having Phe, Tyr, and Trp residues at position $P_1$,[2] but RMCP II showed greater selectivity. In addition, RMCP II is reported to have a lower catalytic rate toward substrates such as Ac-Tyr-OEt (Katunuma et al., 1975). The specificity of human leukocyte cathepsin G has been studied toward both the insulin B chain (Blow & Barrett, 1977) and peptide 4-nitroanilide substrates (Nakajima et al., 1979).

In this paper, we report a kinetic study of the hydrolysis of a series of peptide 4-nitroanilides by the rat mast cell proteases and human cathepsin G. Both rat enzymes are effective proteases toward such substrates. In addition, we have studied

† From the School of Chemistry, Georgia Institute of Technology, Atlanta, Georgia 30332 (N.Y. and J.C.P.), and the Department of Biochemistry, University of Washington, Seattle, Washington 98195 (M.T.E., H.N., and R.G.W.). *Received May 7, 1980.* This research was supported by grants from the National Institutes of Health (HL 18679), the Council for Tobacco Research to the Georgia Institute of Technology, and the National Institutes of Health (GM 15731) to the University of Washington.

[1] Abbreviations used: NA, 4-nitroanilide; Ac, acetyl; Suc, succinyl; Glt, glutaryl; MeO-Suc, methoxysuccinyl; RMCP I, rat mast cell protease I; RMCP II, rat mast cell protease II; NPGB, *p*-nitrophenyl *p*-quanidinobenzoate.

[2] The nomenclature used for the individual amino acid residues ($P_1$, $P_2$, etc.) of a substrate and the subsites ($S_1$, $S_2$, etc) of the enzyme is that of Schechter & Berger (1967).

0006-2960/80/0419-5799$01.00/0 